J Mol Model (2012) 18:3169–3179
DOI 10.1007/s00894-011-1344-5

ORIGINAL PAPER

Theoretical investigation of the enzymatic phosphoryl transfer of β-phosphoglucomutase: revisiting both steps of the catalytic cycle

Brigitta Elsässer · Silvia Dohmeier-Fischer · Gregor Fels

Received: 5 September 2011 / Accepted: 19 December 2011 / Published online: 12 January 2012

Abstract Enzyme catalyzed phosphate transfer is a part of almost all metabolic processes. Such reactions are of central importance for the energy balance in all organisms and play important roles in cellular control at all levels. Mutases transfer a phosphoryl group while nucleases cleave the phosphodiester linkages between two nucleotides. The subject of our present study is the *Lactococcus lactis* β-phosphoglucomutase (β-PGM), which effectively catalyzes the interconversion of β-D-glucose-1-phosphate (β-G1P) to β-D-glucose-6-phosphate (β-G6P) and vice versa via stabile intermediate β-D-glucose-1,6-(bis)phosphate (β-G1,6diP) in the presence of Mg^{2+}. In this paper we revisited the reaction mechanism of the phosphoryl transfer starting from the bisphosphate β-G1,6diP in both directions (toward β-G1P and β-G6P) combining docking techniques and QM/MM theoretical method at the DFT/PBE0 level of theory. In addition we performed NEB (nudged elastic band) and free energy calculations to optimize the path and to identify the transition states and the energies involved in the catalytic cycle. Our calculations reveal that both steps proceed via dissociative pentacoordinated phosphorane, which is not a stabile intermediate but rather a transition state. In addition to the Mg^{2+} ion, Ser114 and Lys145 also play important roles in stabilizing the large negative charge on the phosphate through strong coordination with the phosphate oxygens and guiding the phosphate group throughout the catalytic process. The calculated energy barrier of the reaction for the β-G1P to β-G1,6diP step is only slightly higher than for the β-G1,6diP to β-G6P step (16.10 kcal mol^{-1} versus 15.10 kcal mol^{-1}) and is in excellent agreement with experimental findings (14.65 kcal mol^{-1}).

Keywords β-phosphoglucomutase · Pentacoordinated phosphorane intermediate · Phosphoryl transfer · Reaction mechanism · Transition state search · QM/MM

Introduction

Enzymatic phosphate- and sulfate transfer play essential roles in the metabolism of many biological systems in nature [1–3], and research in this field, therefore, is of continuous interest. Although the most important biological phosphates are phosphate diesters like DNA and RNA, many metabolic intermediates exist as monophosphates and are ubiquitous in the biochemical world. Also, the phosphorylation of proteins is an important control mechanism since the phosphorylated proteins are phosphate monoesters, in which a serine, threonine, tyrosine or a histidine residue is phosphorylated. In addition, aspartate residues can also be phosphorylated and mostly exist as transient intermediates. In contrast to phosphate monoesters phosphorylated aspartates are relatively reactive [1].

The most common examples for the presence of an aspartyl-phosphoenzyme are the α- and β-phosphoglucomutases (PGM). Their enzymatic reaction proceeds through a ping-pong mechanism involving aspartyl-phosphoenzyme (β-PGM-P) and β-D-glucose-1,6-bisphosphate (β-G1,6diP) intermediates and accomplishes a phosphoryl transfer between β-G6P and β-G1P (Fig. 1).

The first experimental results of these reactions were reported by Ray and co-workers [4, 5] who investigated

Electronic supplementary material The online version of this article (doi:10.1007/s00894-011-1344-5) contains supplementary material, which is available to authorized users.

B. Elsässer (✉) · S. Dohmeier-Fischer · G. Fels
Department of Chemistry, University of Paderborn,
Warburgerstr. 100,
D-33098 Paderborn, Germany
e-mail: elsaesse@mail.upb.de

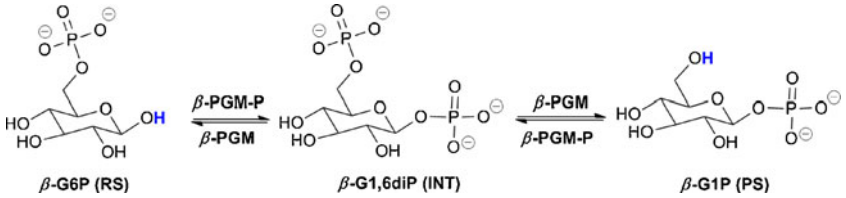

Fig. 1 General mechanism of β-phosphoglucomutase (β-PGM)

the substrate specificity of β-phosphoglucomutase. Ray et al. slowed down the reaction rate to generate "frozen" complexes and analyzed the structures using solvent perturbation difference spectroscopy. They showed that there are two different binding modes for β-G1,6diP that allow phosphoryl transfer of different phosphoryl groups to the enzyme. However, this reaction involves only one catalytic phosphoryl acceptor group. Zhang et al. [6] demonstrated that Asp8 plays an essential role in the catalytic cycle as phosphate acceptor and Asp10 acts as general acid/base. Furthermore, they identified the conformational changes of the enzyme during ligand binding (cap-open, cap-closed), that we also studied by normal mode analysis (see Results and discussion section, Fig. 3). Dai et al. proposed a model [7, 8] to explore the reaction mechanism in which Asp10 plays not only the role of the general acid/base but also is required to stabilize the enzyme in the cap-closed conformation. Using site-directed mutagenesis studies they could assign the roles of other important active site residues like Thr16, His20 and Lys76 which build an extensive hydrogen bond network and thereby strongly contribute to the enzyme stabilization when it changes its conformation as the catalytic reaction proceeds. The crystal structure of β-PGM and glucose-1,6-bisphosphate in the presence of Mg^{2+} at atomic resolution (1.2 Å), elucidated by Lahiri et al. [9] at cryotemperature (PDB Code: 1O08), revealed a pentacoordinated phosphorane intermediate along the reaction pathway. The presence of such pentavalent phosphorane was also confirmed by further experimental studies using MgF_3^- as a transition state analog [10–12]. Furthermore Goličnik et al. performed kinetic analysis and determined the overall reaction rate [11] of the complete catalytic process (Fig. 1). However, they could not assign whether the rate limiting step is defined by the phosphorylation of the sugar or the phosphate cleavage of the bisphosphate. They also found that the bisphosphate (β-G1,6diP) has the highest and β-G1P the lowest affinity to bind to β-PGM and that the equilibrium of the reaction lies strongly toward β-G6P compared with β-G1P.

Based on the crystal structure [9] with the five-coordinated phosphorus, Webster [13] performed DFT/PM3MM calculations considering only the active site and 30 surrounding residues to study the existence of a possible five-coordinated transition state structure using MF_3 and PO_3 as ligands. In addition, the activation energy (14 kcal mol^{-1}) of the β-G6P to β-G1,6diP step was calculated.

In a very recent publication, Marcos et al. [14] studied the pentacoordinated phosphorus along the reaction pathway of the β-G6P to β-G1,6diP step using QM/MM calculations and concluded that the pentacoordinated phosphorane formed during the reaction is not a stable species but rather a transition state and that MgF_3^- proved to be a good transition state analog.

In the present work we have investigated the reaction mechanism of β-phosphoglucomutase and investigated both steps (β-G6P → β-G1,6diP and β-G1,6diP → β-G1P) of the phosphoryl transfer reaction in atomistic detail. In order to generate the enzyme-substrate complex with the reoriented β-G1,6diP we applied docking techniques to predict the structural details. Afterward, we employed a comprehensive quantum mechanical/molecular mechanics (QM/MM) approach to investigate how Asp8 mediates the phosphoryl transfer to and from β-G1,6diP. This study was performed at PBE0/DFT level of theory using the extensive functionality provided by the developed QM/MM [15, 16] modules of the NWChem [17] software package. To fully understand the catalytic mechanism at atomistic detail QM/MM approaches combine a quantum mechanical treatment of those protein groups that are candidates for participating in the chemical reaction with a faster molecular mechanical description of the surrounding protein and solvent environment. Using high level DFT/PBE0 QM/MM calculations with a large QM region (81 atoms) our simulations reveal that starting from the bisphosphate (β-G1,6diP) the catalytic reaction proceeds in both directions via unstable pentacoordinated trigonal bipyramidal phosphorane (see Fig. 2). Starting from β-G6P the first step involves a proton transfer from the sugar O1* oxygen to the general base Asp10. Subsequently, O1* attacks the phosphate of the phosphorylated Asp8 and it undergoes a dissociated [18] inline S_N2-type reaction according to the More O'Ferrall–Jencks plot. Since the obtained pentacoordinated phosphorane (TS1) is not stable the reaction quickly proceeds toward stable intermediate β-G1,6diP. At this point the substrate must leave the active site for reorientation [8] and has to return with the O6*-phosphate group close to Asp8. Due to the absence of crystallographic data of this reoriented structure, the missing coordinates were generated by docking calculations. In the second step, starting from the reoriented bisphosphate (β-G1,6diP) the Asp8 carboxylate attacks the O6*-phosphate and the second trigonal bipyramidal pentacoordinated

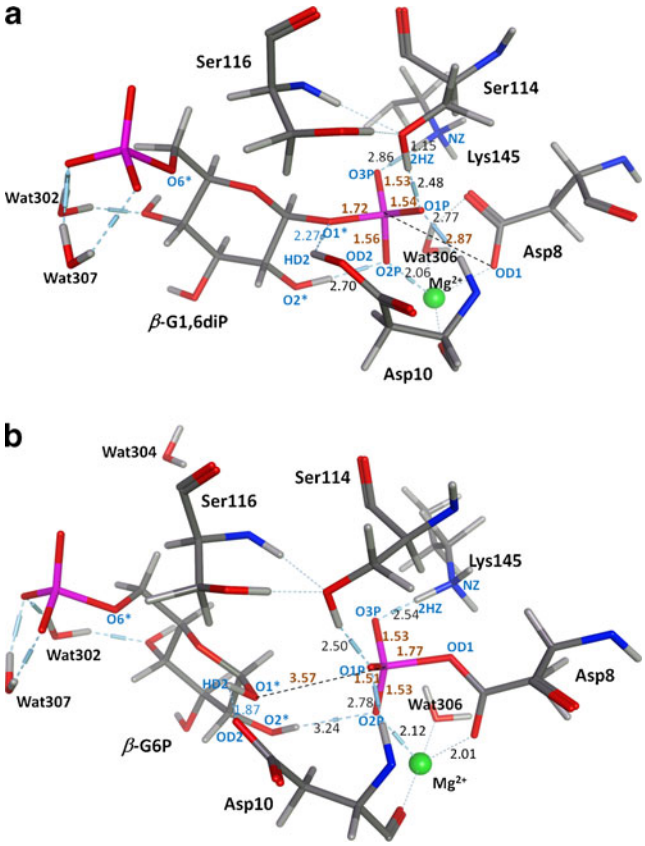

Fig. 2 (left) Stable bisphosphate intermediate (INT) and the active site of β-phosphoglucomutase. (right) β-G6P, QM/MM optimized reactant state. Dashed blue lines indicate H-bonds and black numbers are the corresponding H-bond distances. Brown numbers depict P–O distances. The most relevant atoms are labeled blue. The black dashed line represents the P–OD1(Asp8) distance. The picture was generated by MOE2010.10

phosphorane transition state (TS2) is formed. As a next step the protonated Asp10 acts as a general acid, transfers the proton to O6* to build β-G1P and thereby completes the catalytic cycle. The enzyme requires Mg^{2+} ion for the catalytic activity [3, 19, 20] to neutralize the excess of negative charge of the phosphorane in the transition state. Simultaneously it also positions the bisphosphate substrate in the active site. In addition nudged elastic band (NEB) [21, 22] calculations were performed between the stationary points to identify the transition state structures and analyze the energetics along the reaction coordinates.

This first step of the path is similar to the one suggested by Marcos et al. [14]. However, we describe both steps of the catalytic cycle (β-G6P → β-G1,6diP and β-G1,6diP → β -G1P) and apply a slightly larger QM region (81 atoms) for the NEB calculations and for the single point calculations (126 atoms). This way we are able to compare the reaction rate of both steps. The transition state energy of TS1 and TS2 are comparable, but the bisphosphate intermediate (β-G1,6diP) docks preferably with the O1*-phosphate side close to Asp8.

Computational details and methods

Structural model

The high resolution crystallographic structure of β-phosphoglucomutase from *Lactococcus lactis* (1.2 Å) complexed with a high energy (pentavalent phosphorane) reaction intermediate was used as starting structure for our calculations (PDB code 1O08 [9]). Hydrogen atoms were added to the heavy atoms using Protonate 3D of *MOE 2010.10* [23]. The resulting protonation of the residues are in agreement with the protonation suggested by H++ [24]. Nine sodium ions served as counter ions to maintain neutrality in the system and the complex was solvated in an 80 Å cubic box of water (containing 11832 water molecules) centered on the active site. According to the putative mechanism [2, 19] Asp8 was left unprotonated and Asp10 was protonated at the OD2 oxygen. MD simulations followed by QM/MM optimization showed that the high energy pentacoordinated phosphorane in the crystal structure is unstable since it relaxed to the corresponding bisphosphate during the calculations.

Water molecules

All water molecules present in the crystal structures were included in the calculations. The location of water molecules that can hydrogen bond to a proton donor and/or acceptor is likely to be important for the stabilization of the transition states and intermediates. Based on the above considerations, four water molecules were included in the QM region in all calculations.

Quantum mechanical region

A total of 81 atoms were treated quantum mechanically (QM region). The forces in the QM subsystem were calculated at the DFT/PBE0 level using aug-cc-pVTZ basis set. These comprise fragments of the conserved residues and four additional waters (from the X-ray structure) that potentially stabilize the ligand through H-bonds: Wat302, Wat304, Wat306, Wat307, Asp8, Asp10, Ser114, Ser116, Lys145 (the water molecules HOH3005, HOH3029, HOH3129, HOH3231 were renamed for easier handling). Furthermore, we included the complete substrate (G16) as well as the Mg^{2+} ion.

Mobile region

The remaining protein atoms (2465 atoms), counter ions and the solvent molecules of the water box were included in the molecular mechanics region (MM region) and computationally treated by AMBER99 force field.

MD and QM/MM calculations

The bonds between the QM and MM subsystems were capped with H atoms [15]. In the first step of the calculation the entire solvent-enzyme-substrate structure was equilibrated by performing a series of molecular dynamics annealing runs for 100 ps at temperatures 50 K, 150 K, 200 K, 250 K and 298.15 K with fixed positions of the atoms in the QM region. Afterward, the atomic positions in the MM region were fixed and the atomic positions in the QM region were optimized at the PBE0 level and wavefunctions were expanded using the aug-cc-pVTZ basis set. Then the resulting equilibration stage of the structure was optimized using the multi-region optimization algorithm implemented in NWChem [17]. This method performs a sequence of alternating optimization cycles of the QM and MM regions. The effective charges were recalculated in each optimization cycle by fitting the electrostatic field outside the QM region to that produced by the full electron density representation. Several cycles of this optimization were carried out until convergence was obtained. Single point energy calculations of the reactant, intermediate and product states increasing the QM size (Asp8, Leu9, Asp10, Arg49, Ser114, Ala115, Ser116, Lys117, Lys145, Mg280, Wat302, Wat304, Wat306, Wat307, G16, 126 atoms in total) did not improve our results since the relevant H-bond distances remained almost the same. In addition, our previous calculations [25, 26] on pentacoordinated phosphorus compounds have shown good performance using even a smaller Ahlrichs-pVDZ basis set by describing the geometry and energetics.

Spring method

Starting from the bisphosphate intermediate (β-G1,6diP) a sequence of constrained optimizations were performed to study the phosphoryl transfer. Harmonic restraints (force constant 2.0) between OD1(Asp8) and the phosphorus (1.6 Å) and/or between the phosphorus and the sugar oxygen (O1* or O6*, respectively) were imposed to drive the system over the transition states and reaction barriers to the reactant and product states while at the same time allowing the MM system (initially equilibrated to the reactant structure) to adjust to the changes. When a reasonable estimate of the phosphoryl transfer was obtained, the constraints were lifted, and the system was optimized using a sequence of optimizations and dynamical relaxation steps similar to those discussed above.

NEB calculations

To obtain an unbiased view of the reactive process, we have used the implementation of the NEB approach [21] within the NWChem QM/MM module. The NEB method optimizes the trial reaction pathway between two fixed points. In our simulations we calculated 15-15 replicas (beads) connected by harmonic spring forces between reactant and intermediate and between intermediate product states. To ensure full relaxation of the protein environment, the first NEB optimization pass was followed by 20 ps of molecular dynamics equilibration at room temperature of the MM region for each bead along the pathway. After this equilibration, another round of NEB optimization was performed.

Free energy calculations

The free energy profile over the NEB optimized pathway was obtained by calculating free energy differences between the consecutive NEB beads. This approach is similar to the multilevel perturbation methodology, which has been used by Valiev et al. [27] for reactions in solutions.

Docking calculations

The docking procedure was performed using *MOE 2010.10* [23]. In the potential energy setup panel AMBER99 was chosen as force field. For solvation the implicit model of Born was selected. Two placement methods, alpha triangle and triangle matcher, were employed to find the optimal docking parameters with the result that the alpha triangle method is faster and yields more adequate docking poses. In all cases the scoring was the London dG method and force field refinement was applied allowing for flexibility of the catalytic site within 7.0 Å. Each run was adjusted to retain 30 docked conformations as a cut-off unless fewer suitable poses were found. To evaluate the docking method the QM/MM optimized not reoriented β-G1,6diP was successfully reproduced (RMSD 0.34). The top poses were retained for visual analysis (investigating the H-bond distances, IBAC [28]). The residues Asp8, Leu9, Asp10, His20, Trp24, Lys45, Gly46, Val47, Ser48, Arg49, Lys76, Asn77, Ala 113, Ser114, Ala115, Ser116, Lys117, Asn118, Lys145, Glu169, Asp170 and Ser171 were defined as binding pocket. The desired bisphosphate intermediate for the study of the β-G1,6diP to β-G1P step was constructed by using the "build molecule" panel of MOE and optimized by force field methods (AMBER99) prior to docking. Top hit was optimized as described above in section (e).

Normal mode analysis (NMA)

Upon ligand binding the enzyme undergoes a conformational change following a cap-open cap-closed mechanism. This movement of the enzyme was studied by normal mode analysis using the online servers ElNemo [29] and NOMAD-Ref [30].

The structures of the transition states has also been characterized by frequency calculations using NWChem [17].

Results and discussion

The catalytic action of β-phosphoglucomutase belongs to the neutral nucleophile and anionic leaving group phosphoryl transfer mechanism [31]. This enzyme uses an essential aspartic acid carboxyl function as a nucleophile to form a transient aspartyl phosphate intermediate that donates its phosphoryl group to a second substrate hydroxyl group. The studies of Lahiri et al. [9] established a high energy intermediate along the reaction coordinates. However, the presence of a pentacoordinated phosphorane in the crystal structure was questioned. Previous computational work of Webster [13] and Marcos et al. [14] also suggest that the phosphorane is unstable and rather corresponds to a transition state structure. In agreement with these findings, in our calculation the relaxation and QM/MM optimization of the X-ray structure resulted in the related bisphosphate intermediate (β-G1,6diP). This complex, therefore, was used as the starting point for our studies of the reaction mechanism.

Upon ligand binding the crystallographers observed a conformation change of the enzyme which follows a cap-open, cap-closed mechanism (PDB Codes: 2WHE, 2WF5) [32]. Tama et al. showed that there is a single low-frequency normal mode whose direction compares well with the conformational change and successfully studied the open and closed form of 20 proteins [33]. Using the online servers ElNemo [29] and NOMAD-Ref [30] normal mode analysis was performed to study the cap-open, cap-closed mechanism of β-PGM. The structures of these two conformations are depicted in Fig. 3.

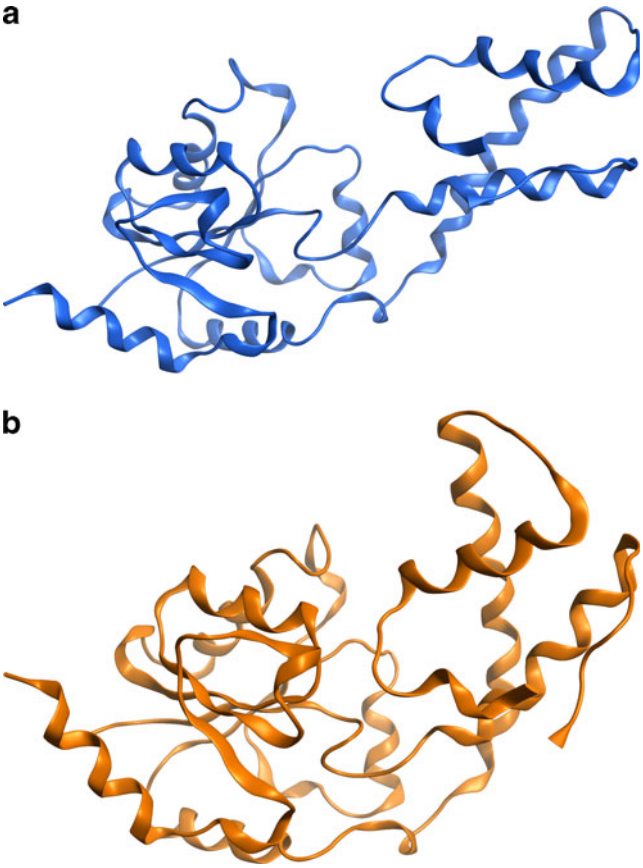

Fig. 3 Open (blue) and closed (orange) conformation of β-PGM

The intermediate to reactant step (β-G1,6diP → (β-G6P)

In the intermediate state (Fig. 2 left) both phosphate groups are covalently bound to the substrate glucose where the closest oxygen (OD1) of the aspartate residue Asp8 is at a distance of 2.87 Å. The large negative charge on the phosphate is stabilized by strong H-bonds to Ser114 (2.48 Å), Lys145 (2.86 Å) and the Mg^{2+}-ion. The OD2 oxygen of Asp10 is protonated and the HD2 proton is ideally positioned to be transferred to O1* during the reaction. The P–O bond is completely formed and has a bond order [34] (BO) of 1.0. To simulate the phosphoryl transfer and to drive the system toward the reactant state β-G6P we applied constraints between the phosphorus and the participating oxygen O1* and OD1(Asp8), respectively. In the first sets of calculation we expanded the P–O1* bond to 2.65 Å to break this bond, as expected, the phosphate was transferred to Asp8. In another separate simulation we used the spring (1.65 Å) to generate a bond between (OD1)Asp8 and the phosphorus. When the calculation converged the phosphate group was carried over to Asp8 and the HD2 proton automatically migrated to O1*. Afterward, the constraints were lifted and the system was QM/MM optimized and it relaxed to the same reactant state β-G6P in both cases. Figure 2 (right) illustrates the reactant state in which the aspartate Asp8 is phosphorylated and the P–OD1 bond is completely formed (BO is 0.86). At this stage OD1(Asp8) is 2.87 Å away from the sugar phosphate. Lys145 still coordinates to O3P with a H-bond length of 2.54 Å and Ser114 is also very strongly H-bonded to O1P (2.50 Å) where NZ(Lys145) and O3P are almost sharing the 2HZ(Lys145) proton since the NZ–2HZ bond length (1.15 Å) is longer than the usual N–H single bond and the 2HZ–O3P distance is 1.40 Å. Furthermore, the O2P oxygen of β-G6P is stabilized by Mg^{2+} and proton of O2*.

In order to achieve a complete overview of the catalytic pathway and to designate the transition state structure and the free energy profile of the reaction we performed NEB calculations between the reactant (β-G6P) and intermediate states (β-G1,6diP). The initial pathway for NEB calculations was calculated by linear interpolation between the reactant and intermediate states of the entire solute-solvent system with 15 beads/replicas for each segment. To support our results the reaction pathway calculations were performed in both directions for both steps and resulted in almost the same structures and energies (see Supporting information).

In this report we describe the reactant to intermediate and intermediate to product direction.

In the reactant to intermediate step there are two important events along the reaction coordinates (Figs. 4 and 5). The first one is the transfer of the proton from O1* to OD2 of the general base Asp10 and the second one is the attack of the phosphate on the O1* oxygen and the formation of the first pentacoordinated phosphorane structure. The magnesium ion plays a predominant role in guiding the phosphate group throughout the catalytic process, since during the phosphoryl transfer the Mg^{2+}–O2P distance remains almost constant (varies between 2.01–2.06 Å). According to our calculation the proton transfer from O1* to OD2(Asp10) occurs fast, at the very beginning of the reaction therefore the energy of the phosphoryl transfer determines the energy barrier and the reaction rate of this step.

This point occurs at the maximum energy along the reaction path (bead 7, 15.10 kcal), when the PO_3^{2-} moiety is shared between the glucose O1* and OD1(Asp8) (TS1, Figs. 4 and 5). For the phosphoryl transfer step the P–OD1 (Asp8) bond expands to 2.23 Å (BO 0.15) and the P–O1* distance is 2.76 Å (BO 0.02). To reach a favored conformation PO_3^{2-} is completely planar at this stage and its P–O bond lengths are equal (1.54 Å). At the transition state the HD2–OD2 bond length is 1.19 Å and the O1*–HD2(Asp10) distance is already as long as 1.66 Å. Afterward, the phosphate transfer continues stepwise. At the intermediate state the phosphoryl transfer to O1* is complete.

The intermediate to product step (β-G1,6diP → (β-G1P)

To continue the catalytic cycle from the intermediate bisphosphate (β-G1,6diP) toward β-G1P product it is required that β-G1,6diP undergoes a reorientation in the pocket. Probably the bisphosphorylated glucose leaves the active site and returns with the O6*-phosphorylated side close to Asp8 which allows the phosphate group to be shuttled to the aspartate residue (Asp8). Zhang et al. [6] identified the conformational changes of the enzyme that occur during catalytic turnover. They found that the catalytic cycle proceeds via "cap-open cap-closed mechanism" as follows: The enzyme opens its active site to bind β-G1,6diP and closes for the transphosphorylation process. Afterward, it opens again to release β-G6P and to absorb β-G1P. Then it is closing again while phosphoryl transfer to O6* takes place and it opens to release β-G1,6diP. The cap domain, which is responsible for opening and closing, comprises the residues: Ser52, Lys79, His20 and Arg49. Their kinetic studies [6] show that the efficiency of enzyme phosphorylation and dephosphorylation is determined by the cap domain, which binds the ligand phosphate group.

In order to investigate the second part (β-G1,6diP → β-G1P) of the phosphorylation reaction by computational approaches reliable starting geometries of the enzyme-ligand complexes are indispensable. Because a crystallographic structure of the reoriented β-G1,6diP is not available in the protein database we applied docking approaches to predicting binding modes of β-G1,6diP ligand inside the active site of the enzyme, i.e., orientation and conformation that allow transfer of the phosphate from O6* to (OD1)Asp8. This procedure has already been shown to successfully regenerate the not reoriented β-G1,6diP with MOE2010 (molecule operating environment) [23]. For evaluation of the docking poses we rather applied the interaction-based accuracy classification (IBAC) method as described by Kroemer et al. [28] since for the reoriented β-G1,6diP-enzyme complex the necessary protein-ligand interactions around the O6*-phosphate are well described in the literature [6, 8, 19]. Therefore, we have determined the correct docking poses by comparing the hydrogen bond (H-bond) lengths and by measuring mechanistically relevant distances between enzyme and bisphosphorylated glucose.

Starting from the QM/MM optimized (not reoriented) β-G1,6diP-enzyme complex the ligand was removed from the active site, bisphosphate was placed then into the pocket with the 6-phosphate side close to Asp8, and the resulting hits were ranked according to their binding energies (London dG scoring function, as implemented into MOE2010). The best docking pose was then optimized in a separate DFT/PBE0 QM/MM simulation (Fig. 6, left) to generate an initial structure for the second set of simulations.

Also in the reoriented intermediate state Lys145 and Ser114 play a significant role to stabilize the negative charge on the phosphate oxygens O1P and O2P. The magnesium ion coordinates as well the O6*-phosphate as the residue Asp8 hereby neutralizing the negative charge on the oxygens

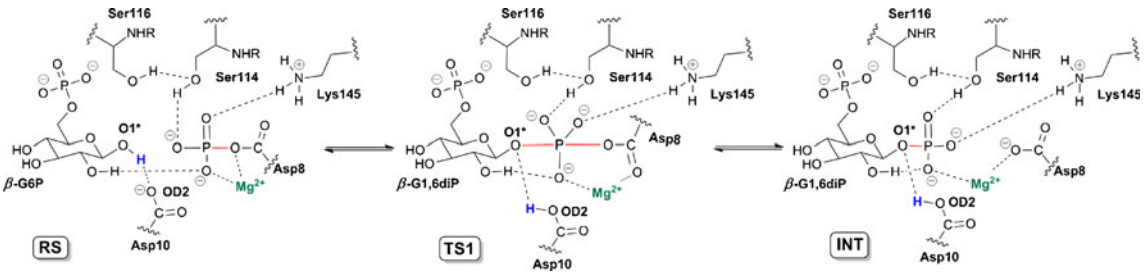

Fig. 4 Proposed reaction mechanism of the intermediate to reactant step (β-G1,6diP → (β-G6P)

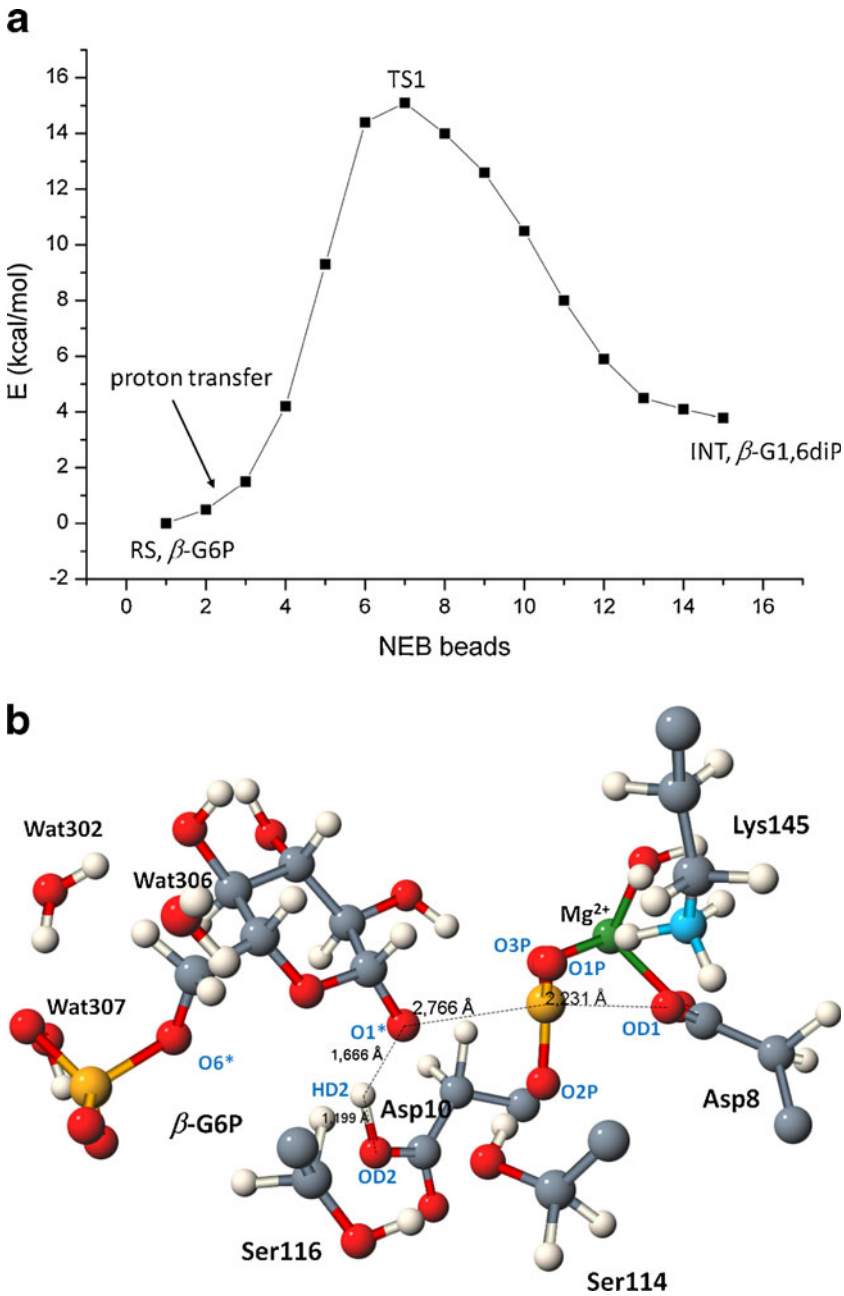

Fig. 5 (left) Calculated free energy profile for the β-G6P → β-G1,6diP phosphoryl transfer of β-PGM. (right) Transition state (TS1) of the reactant to intermediate step. Black numbers indicate the most relevant distances. The curve was generated by Origin7.0 and the picture by Jmol11.0

O3P and O2D(Asp8). In addition O3P is strongly coordinated by Wat305. The P–OD1(Asp8) distance is 2.97 Å and the O6* oxygen is only 1.84 Å away from HD2(Asp10) and is ideally placed for a proton transfer. To proceed with the simulations toward β-G1P (product) the above mentioned spring method was applied. In separate runs harmonic restraints between P–O1D(Asp8) and P–O6* were imposed with a length of 1.65 Å and 2.65 Å, respectively. In both cases the phosphate group has been transferred from O6* to OD1(Asp8) and the HD2(Asp10) proton has automatically shuttled to O6* without setting any forces. QM/MM optimization after removal of the constraints resulted in the same product state structure β-G1P (Fig. 6, right). Similarly to the previous stationary points in the β-G1P state the P–O phosphate bond lengths are almost equal. Partial charges calculations indicate that the negative charge of both phosphate groups is well distributed between the participating oxygens.

All phosphate oxygen atoms are well coordinated by positively charged or proton donor residues, respectively, which stabilize the structure by neutralizing the negative charge.

A detailed overview about the reaction energetics of the β-G1,6diP → β-G1P step and the transition state structure were calculated by the above mentioned NEB method as implemented into NWChem [17]. In this step the reaction proceeds by transferring the O6*-phosphate to OD1(Asp8) and carrying over the HD2(Asp10) proton to O6* to

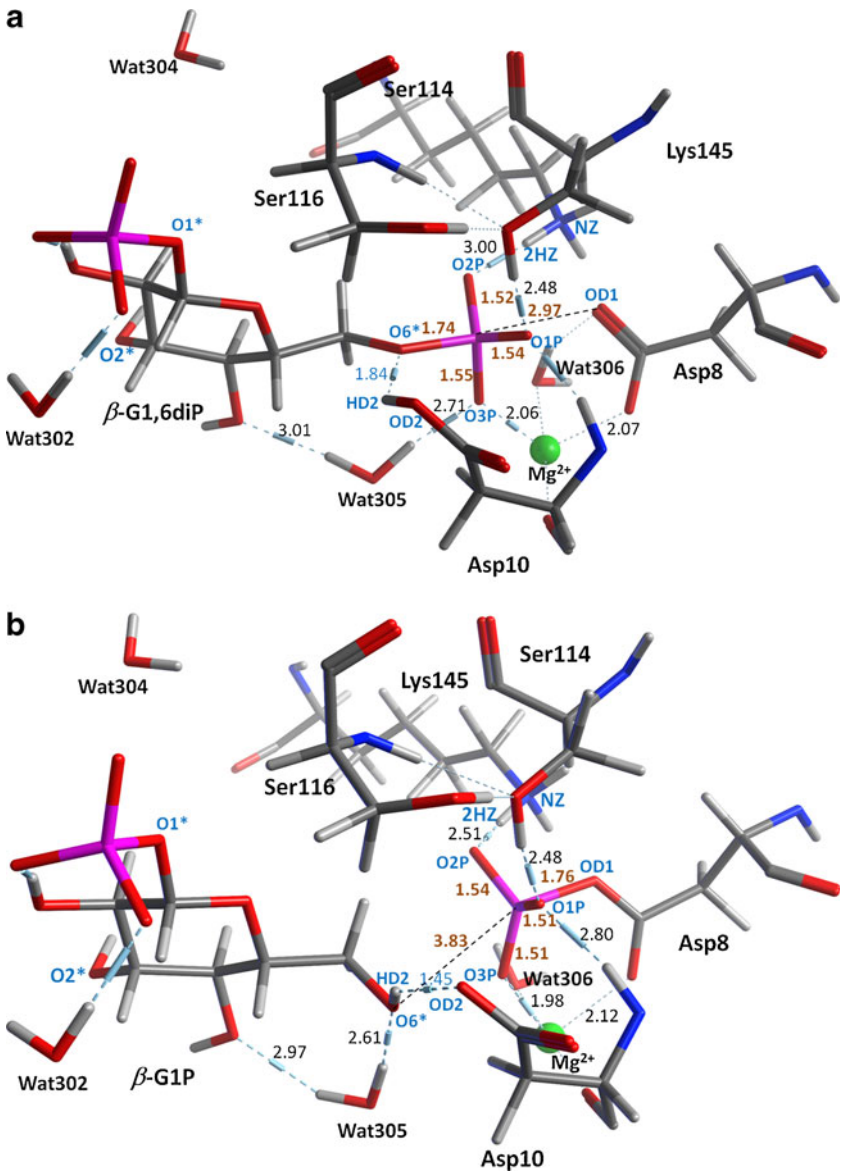

Fig. 6 (left) Structure of the QM/MM optimized reoriented β-G1,6diP in the active site of β-PGM. (right) QM/MM optimized product state, β-G1P, showing the active side residues and the monophosphorylated glucose Dashed blue lines indicate H-bonds and black numbers are the corresponding H-bond distances. Brown numbers depict P–O distances. The most relevant atoms are labeled blue. The black dashed line represents the P-OD1 (Asp8) distance. The picture was generated by MOE2010.10

complete the reaction. Figure 6 shows the QM/MM free energy profile of the intermediate to product step and the structure of the second transition state (NEB bead 6).

In the intermediate to product step the reaction proceeds through a slightly higher reaction barrier (16.10 kcal mol^{-1}, TS2) than for the reactant to intermediate state (15.10 kcal mol^{-1}, TS1). Since in both steps similar phosphoryl transfer takes place it is not surprising that the reaction energies are comparable for both steps and the reaction proceeds through dissociated pentacoordinated phosphorane transition state. Even the geometry of the transition state structures (TS1 and TS2) are very similar (Figs. 5 and 7) because also in TS2 the transferring sugar O–P and P–OD1(Asp8) bonds have a very small bond order of 0.07 and the phosphorane has a trigonal bipyramidal geometry. Also in this step the magnesium ion moves along with the O2P as the reaction proceeds to stabilize the phosphate. The only difference is that in the β-G1,6diP → β-G1P step the proton transfer from HD2(Asp10) occurs later than in the β-G6P → β-G1,6diP step. In TS2 the O6* oxygen and OD2(Asp10) are sharing the HD2 proton, while in TS1 the HD2 proton is already completely transferred to O1*. Normal mode analysis of the transition state structures (TS1 and TS2) show only one negative frequency (see Supporting information), therefore we assume that we could identify the real transition states.

Conclusions

In our study, we present mechanistic details of the reversible enzymatic conversion of β-G6P to β-G1P over β-G1,6diP with β-phosphoglucomutase using hybrid QM/MM methods and docking techniques. We have based our calculation on the high resolution crystal structure of the β-PGM–

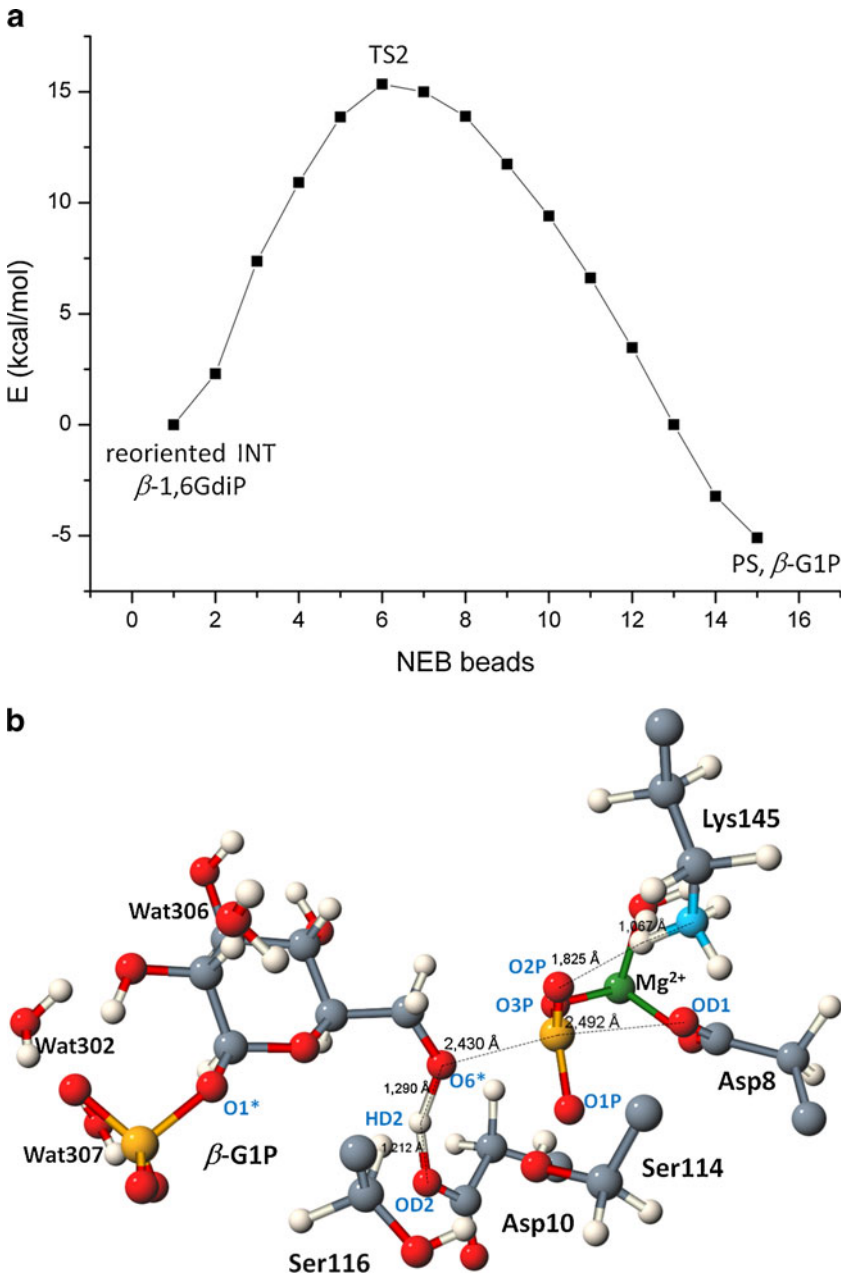

Fig. 7 (left) Calculated free energy profile for the β-G1,6diP → β-G1P phosphoryl transfer of β-PGM. (right) Transition state (TS2) of the reactant to intermediate step. Black numbers indicate the most relevant distances. The curve was generated by Origin7.0 and the picture by Jmol11.0

pentacovalent phosphorus intermediate (TS) complex (PDB code: 1O08) [9]. The most important catalytic site residues comprise Asp8, Asp10, Ser114, Ser116, Lys145 and a magnesium ion. In addition the large numbers of crystal structure water molecules (nine waters) around the ligand build strong H-bond bridges in the active site as well as with the residues and the substrate. The residues Lys145, Ser114 and Mg^{2+} play significant roles in stabilizing the phosphate oxygens and in neutralizing their negative charge and guiding the phosphate group throughout the catalytic process. Starting from the bisphosphate intermediate the phosphoryl transfer from both the O1* and O6* oxygen proceeds to OD1(Asp8) accompanied by a proton transfer from Asp10 to the participating sugar oxygen.

According to our findings the catalytic pathway proceeds via two transition states (TS1 and TS2, Figs. 4 and 6) whose geometries and energy barriers are comparable. After completing the first step the intermediate must leave the catalytic pocket and return after reorientation. Modeling of the reorientation process was not possible since the docking complex needed resolvation which resulted in a different number of solvent molecules as compared to the bisphosphate before reorientation. Due to the unequal number of atoms in the two β-G1,6diP systems no direct energy comparison is possible.

Our study demonstrates how a hybrid QM/MM approach complemented by docking techniques can provide a comprehensive picture of the mechanistic details of a multistep phosphoryl transfer mechanism in a complex chemical

environment. The predictions from the calculations presented in this work expand and differ from earlier studies of Webster [13] and Marcos et al. [14] since we modeled both steps of the catalytic cycle using high level methods and a large QM region. We provide the first reliable theoretical estimate of the reaction free energy for both steps of the catalytic cycle and thereby describe the phosphorylation reaction of β-phosphoglucomutase at atomistic details. Our results yield key insights into the catalytic mechanism of phosphoryl transfer and extend the present knowledge about pentacoordinated phosphorane chemistry.

Acknowledgments The calculations were carried out at the Paderborn Center for Parallel Computing (PC2) and at the Molecular Science Computing Facility in the Environmental Molecular Sciences Laboratory User Facility sponsored by the United Stated Department of Energy. The authors acknowledge Marat Valiev for the normal mode calculations on the transition state structures.

References

1. Cleland WW, Hengge AC (2006) Enzymatic mechanisms of phosphate and sulfate transfer. Chem Rev 106:3252–3278
2. Holmes RR (2004) Phosphoryl transfer enzymes and hypervalent phosphorus chemistry. Acc Chem Res 37:746–753
3. Knowles JR (1980) Enzyme-catalyzed phosphoryl transfer-reactions. Annu Rev Biochem 49:877–919
4. Ma C, Ray WJ (1980) Structural comparisons among the central complexes in the phosphoglucomutase system by means of spectral techniques. Biochem 19:751–759
5. Ray WJ, Long JW, Owens JD (1976) Analysis of substrate-induced rate effect in phosphoglucomutase system. Biochem 15:4006–4017
6. Zhang GF, Dai J, Wang LB, Dunaway-Mariano D, Tremblay LW, Allen KN (2005) Catalytic cycling in beta-phosphoglucomutase: a kinetic and structural analysis. Biochem 44:9404–9416
7. Dai JY, Finci L, Zhang CC, Lahiri S, Zhang GF, Peisach E, Allen KN, Dunaway-Mariano D (2009) Analysis of the structural determinants underlying discrimination between substrate and solvent in beta-phosphoglucomutase catalysis. Biochem 48:1984–1995
8. Dai JY, Wang LB, Allen KN, Radstrom P, Dunaway-Mariano D (2006) Conformational cycling in beta-phosphoglucomutase catalysis: reorientation of the beta-d-glucose 1,6-(bis) phosphate intermediate. Biochem 45:7818–7824
9. Lahiri SD, Zhang GF, Dunaway-Mariano D, Allen KN (2003) The pentacovalent phosphorus intermediate of a phosphoryl transfer reaction. Science 299:2067–2071
10. Baxter NJ, Hounslow AM, Bowler MW, Williams NH, Blackburn GM, Waltho JP (2009) Mgf3- and alpha-galactose 1-phosphate in the active site of beta-phosphoglucomutase form a transition state analogue of phosphoryl transfer. J Am Chem Soc 131:16334–16335
11. Golicnik M, Olguin LF, Feng GQ, Baxter NJ, Waltho JP, Williams NH, Hollfelder F (2009) Kinetic analysis of beta-phosphoglucomutase and its inhibition by magnesium fluoride. J Am Chem Soc 131:1575–1588
12. Tremblay LW, Zhang GF, Dai JY, Dunaway-Mariano D, Allen KN (2005) Chemical confirmation of a pentavalent phosphorane in complex with beta-phosphoglucomutase. J Am Chem Soc 127:5298–5299
13. Webster C (2004) High-energy intermediate or stable transition state analogue: Theoretical perspective of the active site and mechanism of beta-phosphoglucomutase. J Am Chem Soc 126:6840–6841
14. Marcos E, Field MJ, Crehuet R (2010) Pentacoordinated phosphorus revisited by high-level qm/mm calculations. Proteins 78:2405–2411
15. Valiev M, Garrett BC, Tsai MK, Kowalski K, Kathmann SM, Schenter GK, Dupuis M (2007) Hybrid approach for free energy calculations with high-level methods: Application to the s(n)2 reaction of chcl3 and oh- in water. J Chem Phys 127:51102
16. Valiev M, Kawai R, Adams JA, Weare JH (2003) The role of the putative catalytic base in the phosphoryl transfer reaction in a protein kinase: first-principles calculations. J Am Chem Soc 125:9926–9927
17. Valiev M, Bylaska EJ, Govind N, Kowalski K, Straatsma TP, Van Dam HJJ, Wang D, Nieplocha J, Apra E, Windus TL, de Jong WA (2010) Nwchem: A comprehensive and scalable open-source solution for large scale molecular simulations. Comput Phys Commun 181:1477–1489
18. Kamerlin SCL, Florian J, Warshel A (2008) Associative versus dissociative mechanisms of phosphate monoester hydrolysis: on the interpretation of activation entropies. Chemphyschem 9:1767–1773
19. Allen KN, Dunaway-Mariano D, Lahiri SD, Tremblay L, Zhang GF, Dai JY (2004) Mechanism of phosphoryl transfer in a phosphomutase. Abstr Pap Am Chem S 228:U304–U305
20. Kamerlin SCL, Wilkie J (2007) The role of metal ions in phosphate ester hydrolysis. Org Biomol Chem 5:2098–2108
21. Henkelman G, Jonsson H (2000) Improved tangent estimate in the nudged elastic band method for finding minimum energy paths and saddle points. J Chem Phys 113:9978–9985
22. Henkelman G, Uberuaga BP, Jonsson H (2000) A climbing image nudged elastic band method for finding saddle points and minimum energy paths. J Chem Phys 113:9901–9904
23. Moe 2010.10 (http://www.chemcomp.com)
24. Gordon JC, Myers JB, Folta T, Shoja V, Heath LS, Onufriev A (2005) H++: A server for estimating pk(a)s and adding missing hydrogens to macromolecules. Nucleic Acids Res 33:W368–W371
25. Elsaesser B, Valiev M, Weare JH (2009) A dianionic phosphorane intermediate and transition states in an associative a(n) + d-n mechanism for the ribonucleasea hydrolysis reaction. J Am Chem Soc 131:3869–3871
26. Elsaesser B, Fels G (2010) Atomistic details of the associative phosphodiester cleavage in human ribonuclease h. Phys Chem Chem Phys 12:11081–11088
27. Valiev M, Yang J, Adams JA, Taylor SS, Weare JH (2007) Phosphorylation reaction in capk protein kinase-free energy quantum mechanical/molecular mechanics simulations. J Phys Chem B 111:13455–13464
28. Kroemer RT, Vulpetti A, McDonald JJ, Rohrer DC, Trosset JY, Giordanetto F, Cotesta S, McMartin C, Kihlen M, Stouten PFW (2004) Assessment of docking poses: interactions-based accuracy classification (ibac) versus crystal structure deviations. J Chem Inf Comput Sci 44:871–881
29. Suhre K, Sanejouand YH (2004) Elnemo: A normal mode web server for protein movement analysis and the generation of templates for molecular replacement. Nucleic Acids Res 32: W610–W614
30. Lindahl E, Azuara C, Koehl P, Delarue M (2006) Nomad-ref: visualization, deformation and refinement of macromolecular

structures based on all-atom normal mode analysis. Nucleic Acids Res 34:W52–W56
31. Bowler MW, Cliff MJ, Waltho JP, Blackburn GM (2010) Why did nature select phosphate for its dominant roles in biology? New J Chem 34:784–794
32. Baxter NJ, Bowler MW, Alizadeh T, Cliff MJ, Hounslow AM, Wu B, Berkowitz DB, Williams NH, Blackburn GM, Waltho JP (2010) Atomic details of near-transition state conformers for enzyme phosphoryl transfer revealed by mgf(3)(-) rather than by phosphoranes. Proc Natl Acad Sci USA 107:4555–4560
33. Tama F, Sanejouand YH (2001) Conformational change of proteins arising from normal mode calculations. Protein Eng 14:1–6
34. Berente I, Beke T, Naray-Szabo G (2007) Quantum mechanical studies on the existence of a trigonal bipyramidal phosphorane intermediate in enzymatic phosphate ester hydrolysis. Theor Chem Acc 118:129–134